Remdesivir

Ahmed H. Bakheit[a,b], Hany Darwish[a], Ibrahim A. Darwish[a], and Ahmed I. Al-Ghusn[a]

[a]Department of Pharmaceutical Chemistry, College of Pharmacy, King Saud University, Riyadh, Kingdom of Saudi Arabia
[b]Department of Chemistry, Faculty of Science and Technology, Al-Neelain University, Khartoum, Sudan

Contents

1. Description

Remdesivir (GS-5734) is the first medication for severe coronavirus disease that was approved by the FDA in 2019 (COVID-19). It is a novel nucleoside analog with broad antiviral activity against a wide range of RNA viruses, including ebolavirus (EBOV) and respiratory pathogens like Middle East respiratory syndrome coronavirus (MERS-CoV), SARS-CoV, and SARS-CoV-2 [1]. Remdesivir, a single diastereomer monophosphoramidate as a prodrug, is converted into the active form GS-441524 after administration. GS-441524 competes with ATP for RNA incorporation and inhibits viral RNA–dependent RNA polymerase. This stops RNA transcription and reduces viral RNA replication [2].

1.1 Nomenclature

1.1.1 IUPAC name

- 2-ethylbutyl (2S)-2-[[[(2R,3S,4R,5R)-5-(4-aminopyrrolo[2,1-f][1,2,4] triazin-7-yl)-5-cyano-3,4-dihydroxyoxolan-2-yl]methoxy-phenoxyphosphoryl]amino]propanoate [3].
- 2-ethylbutyl (2S)-2-{[(S)-[(2R,3S,4R,5R)-5-{4-aminopyrrolo[2,1-f] [1,2,4]triazin-7-yl}-5-cyano-3,4-dihydroxyoxolan-2-yl]methoxy (phenoxy)phosphoryl]amino}propanoate [4].

1.1.2 Non-proprietary names (generic names) [5]

- Remdesivir
- Remdesivirum
- GS 5734
- UNII–3QKI37EEHE
- 2-ethylbutyl (2S)-2-(((2R, 3S, 4R, 5R)-5-(4-aminopyrrolo(2,1-f) (1,2,4)triazin-7-yl)-5-cyano-3,4-dihydroxytetrahydrofuran-2-yl) methoxy) (phenoxy) phosphoryl) amino) propanoate [6].

- L–Alanine, N-((S)-hydroxyphenoxyphosphinyl)–, 2-ethylbutyl ester, 6-ester with 2-C-(4-aminopyrrolo(2,1-f)(1,2,4)triazin-7-yl)-2,5-anhydro-d-altrononitrile [7].
- (2S)-2-{(2R,3S,4R,5R)-[5-(4-aminopyrrolo[2,1-f][1,2,4]triazin-7-yl)-5-cyano-3,4-dihydroxy-tetrahydro-furan-2-ylmethoxy]phenoxy-(S)-phosphorylamino}propionic acid 2-ethyl-butyl ester [7].
- 2-ethylbutyl N-[(S)-{[(2R,3S,4R,5R)-5-(4-aminopyrrolo[2,1-f][1,2,4]triazin-7-yl)-5-cyano-3,4-dihydroxytetrahydrofuran-2-yl]methoxy}(phenoxy)phosphoryl]-L-alaninate [7].
- 2-Ethylbutyl (2S)-2-{[(S)-{[(2R,3S,4R,5R)-5-(4-aminopyrrolo[2,1-f][1,2,4]triazin-7-yl)-5-cyano-3,4-dihydroxytetrahydro-2-furanyl]methoxy}(phenoxy)phosphoryl] amino}propanoate [8].

1.1.3 Proprietary names (brand names)
- Veklury [9].

1.2 Formula
1.2.1 Empirical formula, molecular weight, CAS number
The empirical formula, molecular weight, and CAS number of vandetanib are shown in Table 1.

1.2.2 Structural formula
A representation of the two-dimensional structural formula of Remdesivir may be seen in Fig. 1.

1.2.3 Elemental analysis
See Table 2.

Table 1 Empirical formula, molecular weight, CAS number [5].

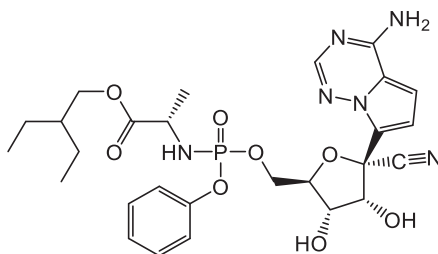| Compounds	Empirical formula	Molecular weight	CAS number
Remdesivir	$C_{27}H_{35}N_6O_8P$	602.6	1809249–37–3

Fig. 1 Chemical structure of Remdesivir.

Table 2 Remdesivir's theoretical elemental analysis and composition were presented in Table 2 [3,5].

Elements	Remdesivir (%)
C	53.82
H	5.85
N	13.95
O	21.24
P	5.14

2. Methods of synthesis

Siegel et al. [10] synthesized a single Sp phosphoramidate prodrug (Remdesivir) by combining comp **6** with glycosylation via metal–halogen exchange of the bromo-base **3** followed by addition into the ribolactone **2** (Scheme 1). Two conditions were identified that resulted in the creation of the required C–C bond. The first condition (a) was achieved by adding excess n–BuLi to a solution of TMSCl and **3**, which was expected to result in lithium–halogen exchange following silyl protection of the acidic 6N protons. After adding this in situ produced reagent to the ribolactone **2**, **4** was obtained in a 25% yield. In the alternate condition (b), sodium hydride and 1,2–bis(chlorodimethylsilyl)ethane were used to guard the 6N atoms, followed by lithium-halogen exchange and addition to the lactone to get **4** in 60% yield. Both conditions were inefficient since the yields were highly variable and greatly reliant on the cryogenic temperatures and rate of n–BuLi addition required for the transformation. Additionally, we observed premature quenching and reduction of lithio base, which was explained as a result of alpha deprotonation to the lactone under very basic circumstances. Compound **4** was separated as a mixture of 1′-isomers that were then used in the subsequent 1′-cyanation procedure to obtain the primary product, -anomer **5**. After removing the three benzyl protecting groups to obtain **6**, the diastereomeric combination of the phosphoramidoyl chloridate prodrug moiety **7** was linked to generate 1a in a yield of 21% as a 1:1 diastereomeric mixture.

The synthetic approach proposed by Gilead scientists for commercial manufacturing of Remdesivir entails protecting group modifications of
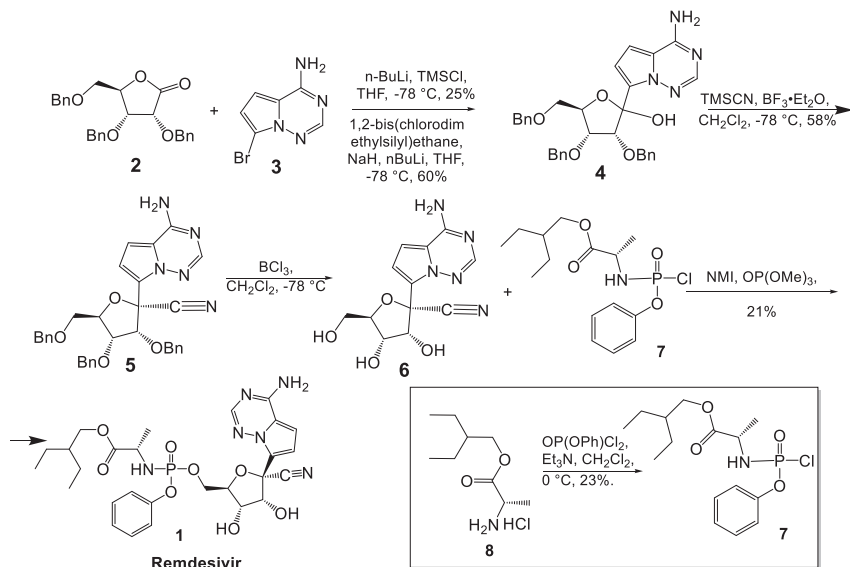
Scheme 1 Siegel route for synthesis of Remdesivir.

the sugar portion during the synthesis, allowing for further optimization [11,12]. The conversion of D–ribose (**2**) to 2,3,5–tri–O–benzyl–D–ribonolactone (**3**), followed by the addition of the modified nucleobase 4–amino–7–iodopyrrolo[2,1–f][1,2,4]triazine (**4**) to the lactone, yielded the C–glycosylated product **5**. BCl₃ was used to remove all three benzyl groups from the triol, and the two secondary alcohols were then protected as isopropylidene ketal **7** after the cyanation process to product **6**. When phosphate ester **8** is added to ketal **7** after hydrolysis, it forms Remdesivir (1) (Scheme 2).

Kumar Palli et al. [12] developed a short synthetic route to Remdesivir in seven longest linear steps with a total yield of 25% starting from D–ribonolactone **2** (Scheme 3A and B). The process involves silylating the primary hydroxyl group of commercially available D–ribonolactone (**2**, which can alternatively be produced in one step from D–ribose), using *tert*–butyldiphenyl silyl (TBDPS) to yield the corresponding silyl ether **3** in 84% yield. Additional protection of the remaining two secondary alcohols with allyl *tert*–butyl carbonate **4** in the presence of 2 mol% Pd(PPh₃)₄ resulted in 89% yield of diallylated ribonolactone **5** (Scheme 3A). Following that, lactone **5** was C–glycosylated with the protected nucleobase tert–butyl(7–bromopyrrolo [2,1–f] [1,2,4] triazin–4–yl) carbamate **6**, which produced an anomeric
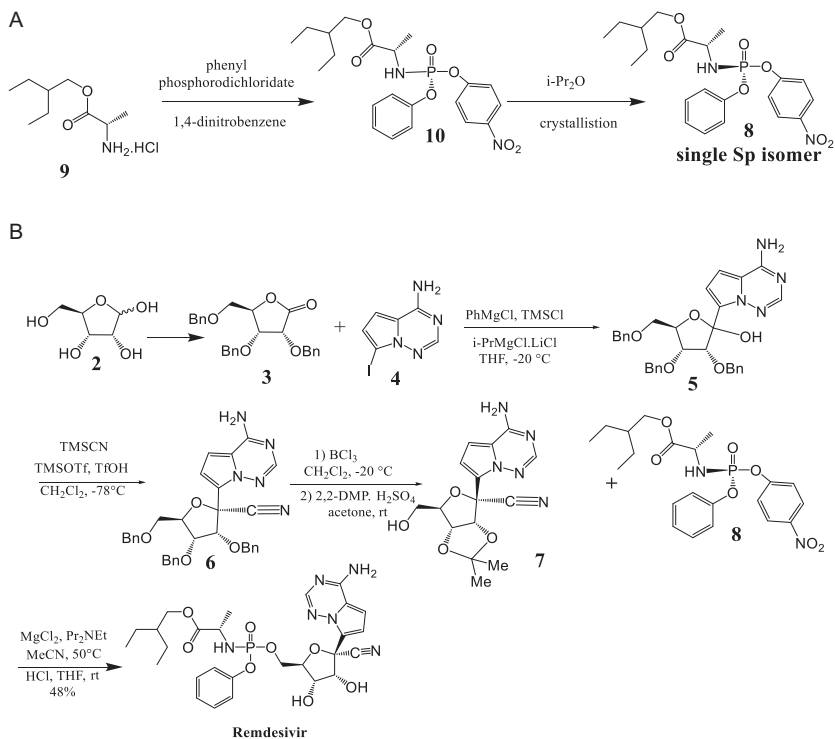
Scheme 2 (A) Synthesis of a single Sp isomer **8** from a *p*-nitrophenolate prodrug precursor **10** instead of phenyl phosphorodichloridate afforded. (B) Gilead route for the synthesis of Remdesivir (**1**, GS-5734).
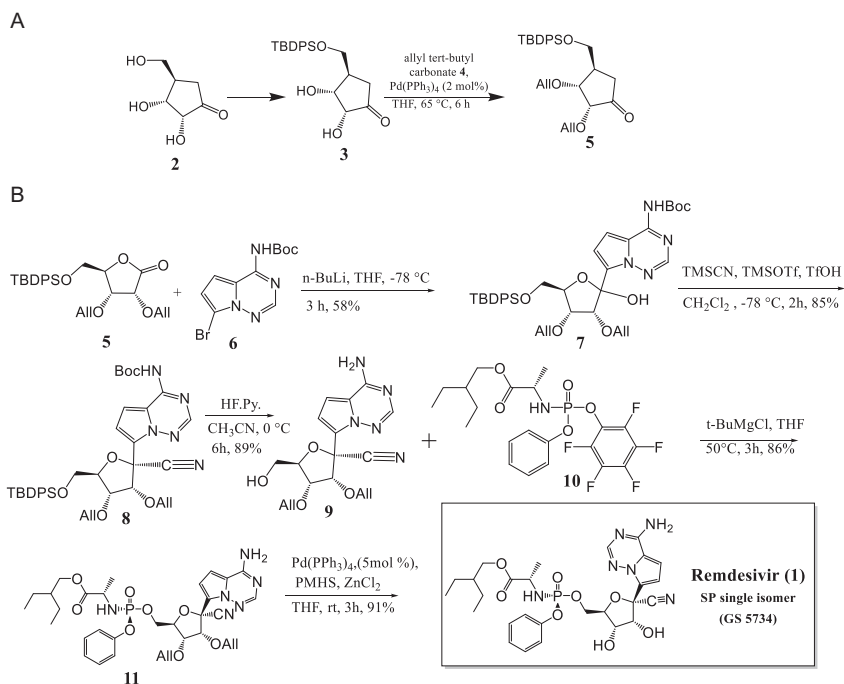
Scheme 3 (A) Synthesis of 5-*O*-TBDPS-2,3-*O*-diallyl ribonolactone **5.** (B) Total synthesis of remdesivir (**1**, *GS-5734*).

combination (2:1) of C-glycosylated product **7** in 58% yield in the presence of n–BuLi. Under standard conditions, cyanation of **7** produced cyano-glycoside **8** in an 85% yield with high selectivity for the target isomer (d.r. = 96:4, β:α). To insert the required phosphonate on the primary hydroxyl group, the silyl and Boc groups were deprotected in one–pot using HF. Pyridine to give amino-alcohol **9** in 89% yield. The following step was P-chiral phosphorylation, a critical step in the production of Remdesivir. The coupling reaction of **9** with the known chiral pentafluoro-phosphoramidate **10** in the presence of t-BuMgCl led to formation of the phosphoramidate ester **11** in an 86% yield as a single diastereoisomer.

3. Physical characteristics
3.1 Physical description

Remdesivir is made up of a non-hygroscopic crystalline solid that comes in a range of colors from white and off-white to yellow [13].

3.2 Dissociation constants

pK_a (strongest acidic/basic) = 10.23/0.65 [2].

3.3 Solubility characteristics

Remdesivir is soluble in ethanol and completely soluble in methanol. It is virtually insoluble in water and its aqueous solubility is pH dependent, increasing as the pH drops; It is very slightly soluble in water when pH is adjusted to pH 2 using HCl [13].

3.4 Partition coefficient

Log Po/w = 2.01 [2].

3.5 Particle morphology
3.5.1 Single crystal structure

Sekharan et al. [14] demonstrated a stable solid of Remdesivir form in a short period of time using the microcrystal electron diffraction (MicroED) technology and a cloud-based and artificial intelligence-based crystal structure prediction platform.

In agreement with experimental findings, the MicroED structures of Remdesivir forms II and IV were shown, and it was found that form

II is more stable at room temperature than form IV. Diffraction data were collected from ten distinct Remdesivir form II crystals, each of which covered $\sim 30°$ of reciprocal space. To eliminate diffractions with a low signal–to–noise ratio, the resolution was limited to $0.900\,\text{Å}$. The combined data set contains 11 574 total diffractions and 3562 individual diffractions, with a 91% completeness rate and a Rint value of 0.2297. The observed symmetry of the diffraction intensity is 2/m Laue, indicating that the Remdesivir form II crystal is monoclinic. With the P21 space group, the unit-cell constants are $a = 10.21(4)\,\text{Å}$, $b = 12.49(14)\,\text{Å}$, $c = 10.85(10)\,\text{Å}$, $\alpha = 90°$, $\beta = 100.9(6)°$, $\gamma = 90°$. Generally, the experimental structures were identified in the CSP landscape, which was used for validation by comparing the predicted structures from the calculation of XRDs. In the Remdesivir landscape, there are 35 crystal polymorphs predicted, with 22 belonging to the P21 space group, eight to the P212121 space group, and five to the P1 space group. Within a relative lattice energy gap of $10\,\text{kJ mol}^{-1}$, only three crystal polymorphs (X1, X2, X3) belonging to the P21 space group are discovered. The comparison of predicted and experimental XRPD patterns, as well as the RMSD15 structural overlays, indicate that X1 and X2 are the experimental structures corresponding to forms IV (RMSD $= 0.368$) and II (RMSD $= 0.441$), respectively. In comparison to X1, the most dramatic stabilization occurs for X2, which loses over $5\,\text{kJ mol}^{-1}$ of energy to become more stable than X1 at room temperature, consistent with experimental data. At $300\,\text{K}$, the difference in the amount of energy between X1 and X2 is $0.76\,\text{kJ mol}^{-1}$, which is within the CSP calculations' estimated range of $1.5\,\text{kJ mol}^{-1}$ for the energy difference. There are two polymorphs, and it's hard to tell which one is the most stable based on the results of the CSP test alone. The free energy calculations show that there isn't a stable form that hasn't been found yet. So, when choosing a stable solid form of Remdesivir, you should look at the competitive slurry tests between polymorphs II and IV. It looks like form II (X2) is the most stable solid form of Remdesivir.

Yu et al. [15] used A Bruker D8 Quest CCD diffractometer with Ga Kα ($=1.341\,\text{Å}$) and a Bruker Apex-II CCD diffractometer with Mo Kα ($= 0.7107\,\text{Å}$) to get the crystal data for RDV-I and RDV-II. On data reduction, the SAINT V8.38A program was employed. The absorption adjustment was carried out using the SADABS program's semi-empirical methods. Direct methods were used to figure out the crystal structures.

They were then refined with full–matrix least–squares methods with anisotropic thermal parameters for all non–hydrogen atoms on F^2 using SHELXL–2016. An isotropic riding model was used to refine hydrogen atoms in the location of calculation after they were placed in the position of calculation. Refinement of the crystal structure of RDV–I: The two alkane chains that were attached to C22A and C22B had a lot of conformational disorder. Their relative ratios of 0.45/0.55 and 0.47/0.53 were fine–tuned for the disordered areas. The structure is twinned around the (1 0 0) lattice direction. The twin matrix was suggested by the ROTAX program, and the HKLF 5 type file was made with the MAKE HKLF5 tool in the WinGX suite. Two twinned domains' ratios were fine–tuned to 0.58/0.42.

Single crystal X–ray structure analysis showed that RDV–I and RDV–II crystallize in the *P1* and *P2₁* groups, respectively (Table 3). RDV–asymmetric I's unit has two RDV molecules, whereas RDV–asymmetric II's unit contains only one RDV molecule. In a structure overlay, you can see that the two RDV molecules in RDV–I have the same conformation, but RDV–II has a very different conformation from that of RDV–I. They have a lot of flexibility because there are single bonds, which allows them to move around in different ways. This is especially true of the three bonds around the phosphorus centers that have single bonds.

3.5.2 X-ray powder diffraction pattern

Sahakijpijarn et al. [16] evaluated the powders' crystallinity using a benchtop X-ray diffraction apparatus (Rigaku Miniflex 600 II, Woodlands, TX, USA) equipped with primary monochromated radiation (Cu K radiation source, $\lambda = 1.54056$). The instrument was run at a 40 kV accelerating voltage and a current of 15 mA. Samples were placed into the sample holder and scanned in continuous mode at a scan speed of 2°/min and a dwell period of 2 s with a step size of 0.02 degree over a 2θ range of 5–40 degree. The X-ray diffraction patterns of Remdesivir powder formulations with thin film freezing (TFF) are provided different results. There were no strong peaks identified in any of the formulations, indicating that Remdesivir was amorphous following the (TFF) procedure. The drug loading and co-solvent type had no effect on Remdesivir's morphology. For excipients, high peaks of mannitol (13.5, 17, 18.5, 20.2, 21, 22, 24.5, 25, 27.5, and 36 degree two-theta) were detected in a number of crystallizations, showing that mannitol

Table 3 Relevant crystallographic data for **Remdesivir-I** and **II**.

Crystal data	Remdesivir-I	Remdesivir-II
Chemical formula	$C_{27}H_{35}N_6O_8P$	$C_{27}H_{35}N_6O_8P$
M_r	602.58	602.58
Crystal system, Space group	Triclinic, $P1$	Monoclinic, $P2_1$
Temperature (K)	170(2)	170(2)
a, b, c (Å)	8.5565(11), 10.5456 (16), 17.147(2)	10.5286(17), 12.809(2), 11.1106(19)
α, β, γ (°)	96.105(4), 99.219(4), 94.937(4)	90, 100.022(5), 90
Volume (Å^3)	1510.1(4)	1475.6(4)
Z, $D_c/(g/cm^{-3})$	2, 1.34139	2, 1.356
Radiation type	GaKα	MoKα
F(000)	636	636
Data collection		
T_{min}, T_{max}	0.5372, 0.7508	0.4799, 0.7455
μ (mm^{-1})	0.837	0.152
Measured, and independent	24511, 24511	28620, 6455
Observed reflections	9621	5990
Flack parameter	0.09(4)	$-0.01(4)$
R_{int}	0.1356	0.0606
Refinement		
$R[F^2 > 2\sigma(F^2)]$	0.0885	0.0572
$wR(F^2)$	0.2506	0.1538
S	0.998	1.077
No. of refined parameters	860	384
$\Delta\rho_{max}$ (e Å^{-3})	-0.339	-0.332
$\Delta\rho_{min}$ (e Å^{-3})	0.299	0.961

remained crystalline as a mixture of δ and α form in these formulations [17]. Similarly, certain leucine peaks (6 and 19 degree two-theta) were identified in all crystallized TFF Remdesivir–leucine formulations, demonstrating that leucine retained its crystallinity during the procedure. Captisol® and lactose, on the other hand, remained amorphous during the TFF procedure.

4. Thermal methods of analysis
4.1 Melting behavior

The melting enthalpy heat-flow curves for the Remdesivir at 127 and 137 °C, respectively, clearly demonstrate the crystalline character of the material [16,18].

4.2 Differential scanning calorimetry

Sahakijpijarn et al. [16] performed thermal analysis of powder samples using a differential scanning calorimeter Model Q20 fitted with a refrigerated cooling system (TA Instruments Inc., New Castle, DE, USA) (RCS40, TA Instruments Inc., New Castle, DE, USA). Samples weighing 2–3 mg were weighed and placed into a T-zero pan to be used later. Before placing the pan in the sample holder, the T-zero hermetic cover was crimped and a hole bored in the lid. To determine the glass transition temperature and glass-forming capabilities of unprocessed Remdesivir powder, samples were heated at a rate of 10 °C/min from 25 to 150 °C, cooled to 40 °C, and then heated to 250 °C. To determine the crystallinity of the TFF formulations, samples were heated from 25 to 350 degrees Celsius at a rate of 5 °C/min. The scans were conducted with a modulation period of 60 s and an amplitude modulation of 1 °C. Throughout the analysis, dry nitrogen gas at a flow rate of 50 mL/min was utilized to cleanse the DSC cell. TA Instruments Trios V.5.1.1.46572 software was used to process the data (TA Instruments, Inc., New Castle, DE, USA).

Modulated differential scanning calorimetry (mDSC) was used to measure Remdesivir's glass-forming ability and glass transition temperature (Tg) in each formulation. The mDSC thermogram of Remdesivir unprocessed powder is shown peak with enthalpy 103.56 J/g°C. The initial heating cycle established that Remdesivir was crystalline and possessed a melting

point of 133 °C. The cooling and second heating cycles revealed that Remdesivir's glass transition temperature was around 60 °C. In no cycle was a recrystallization peak seen.

Yu et al. [15] performed thermal analysis on RDV-I and RDV-II samples using a differential scanning calorimeter (TA DSC Q100). A powder sample weighing approximately 2.4 mg was placed in an aluminum pan and heated at a rate of $10\,°C\,min^{-1}$ with a nitrogen flow rate of 50 mL. min^{-1} over a temperature range of 20–200 °C. DSC analysis showed that RDV-II is a more thermodynamically stable polymorph.

4.3 Thermogravimetric analysis

Thermal Gravimetric Analysis (TGA) of Remdesivir was obtained using a Perkin Elmer pyris 1 apparatus. The sample (2.042 mg) were placed in Aluminum pan, pierced prior to scan, and temperature profile 50–550 °C at a rate of 10 °C/min under nitrogen purge (50 mL/min). Gravimetric Analysis (TGA) can be seen that the powder of Remdesivir is chemically unstable above the melting point temperatures and the compound was decomposing at 199 °C. as shown in Fig. 2.
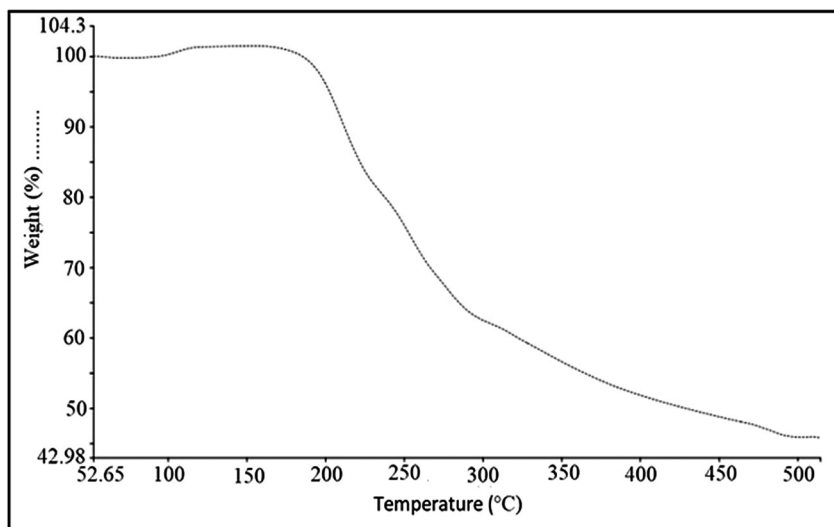

Fig. 2 Thermogravimetric analysis (TGA) of Remdesivir.

5. Characterization and identification

5.1 Spectroscopy

5.1.1 UV/Vis spectroscopy

A Shimadzu UV–spectrophotometer (model no. UV-1800) was used to record an ultraviolet absorption spectrum of Remdesivir (20 μg/mL) in methanol. The absorption spectra are measured in a 1 cm quartz cell within 200–400 nm range. The ultraviolet spectrum is displayed in Fig. 3 with two a maximum absorption of Remdesivir at 210 and 240 nm.

5.1.2 Spectrofluorometry

The fluorescence spectrum emission of Remdesivir in methanol was recorded using a Jasco FP-8200 Spectrofluorometry (Jasco Corporation, Japan) equipped with a 150 W xenon lamp and 1 cm quartz cells. The slit widths for both the excitation and emission monochromators were set at 5.0 nm. Remdesivir exhibited maximum excitation at 245 and maximum emission at 402 nm. The fluorescence spectrum of Remdesivir is shown in Fig. 4.

5.1.3 Infrared spectroscopy

The infrared absorption spectrum of Remdesivir was recorded as KBr disk using the Perkin Elmer FT-IR Spectrum BX apparatus. Fig. 5 showed the FT-IR of Remdesivir. The characteristic absorption bands are shown in Table 4.
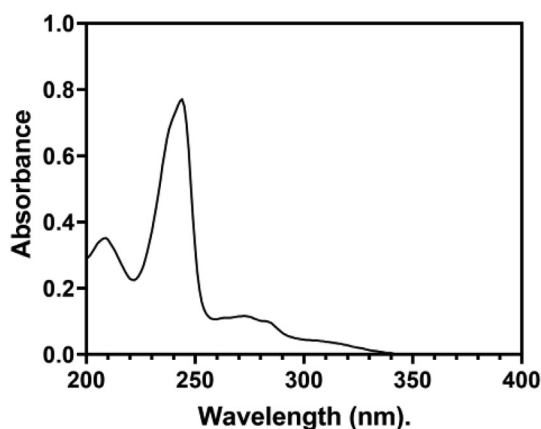
Fig. 3 The UV-absorption spectrum of 20 μg/mL of Remdesivir in methanol.
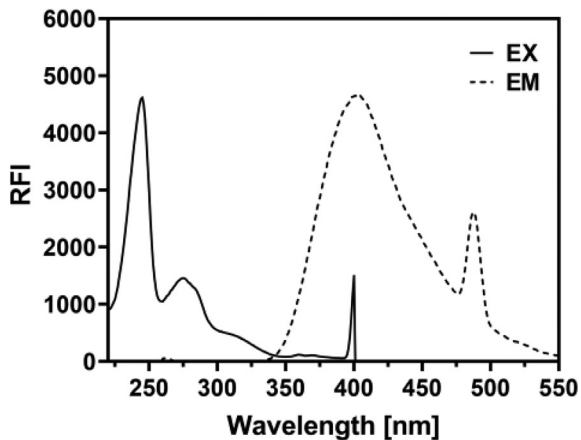
Fig. 4 The fluorescence spectrum excitation and emission of Remdesivir in methanol.
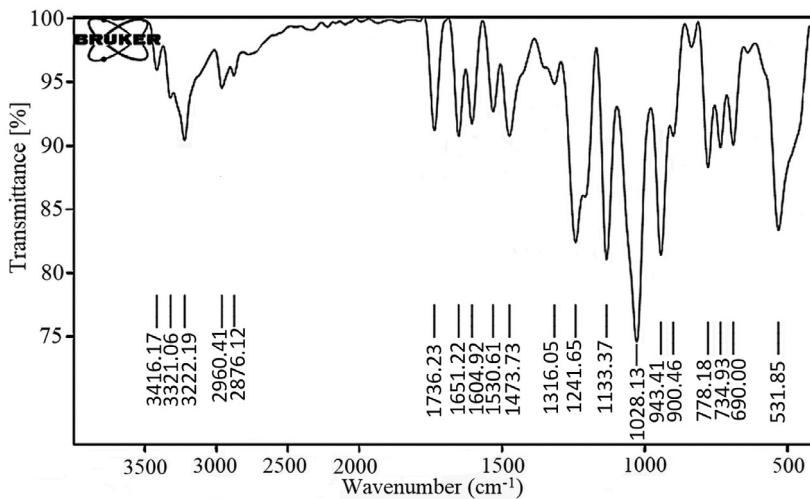
Fig. 5 IR spectrum of Remdesivir.

Table 4 Interpretation of Remdesivir FTIR spectra.

No.	Functional group	Standard value (cm^{-1})	Obtained value
1	C—O group	1050–1150	1133.37
2	C—N group	1000–1350	1241.65
3	C=C group	1600–1680	1604.92
4	C=O group	1640–1810	1736.23
5	C—H group	2850–3000	2960.41
6	O—H group	2500–3400	3222.19
7	N—H group	3300–3500	3416.17

5.1.4 Nuclear magnetic resonance spectrometry

5.1.4.1 ^{1}H NMR spectrum

^{1}H NMR spectrum of Remdesivir was scanned in DMSO-d6 on a Brucker NMR spectrometer operating at 500 MHz. Chemical shifts are expressed in δ-values (ppm) relative to TMS as an internal standard. Coupling constants (J) are expressed in Hz (Table 5 and Fig. 6).

5.2 Mass spectrometry

The mass spectrum of Remdesivir ($C_{27}H_{35}N_6O_8P$, 602.6) was obtained using an Agilent 6320 Ion trap mass spectrometer (Agilent technologies, USA) equipped with an electrospray ionization interface (ESI). A connector was used instead of a column. Mobile phase composed of a mixture of solvents A and B (50:50), where A is HPLC grade water, and B is acetonitrile. The compound was prepared by weighing the solid substances to $1 mg mL^{-1}$ in DMSO and diluted with mobile phase. The test solution was prepared by diluting the stock solutions to $10–30 mg mL^{-1}$ depending

Table 5 ^{1}H NMR of Remdesivir (DMSO-d6).

Signal	Location (δ)	Shape	Integration	Correspondences
1	7.93	s	2	$Ar—NH_2$
2	7.34	m	2	ArHs
3	7.18	m	3	ArHs
4	6.90	s	1	Pyrimidine—H
5	6.22	d	1	Pyrrole—Hs
6	6.34	d	1	Pyrrole—Hs
7	6.04	d	1	—OH
8	5.38	d	1	—OH
9	4.66	t	1	—NH—
10	4.25	m	3	Furan—Hs
11	4.09	t	2	$CH_2—O—C=O$
12	3.96	m	2	$CH_2—O—P=O$
13	3.86	m	1	—CH—C=O
14	1.42	m	1	$—CH—(CH_2—CH_3)_2$
15	1.26	m	7	$—(CH_2)_2—$, $—CH—CH_3$
16	0.78	td	6	$—CH—(CH_2—CH_3)_2$
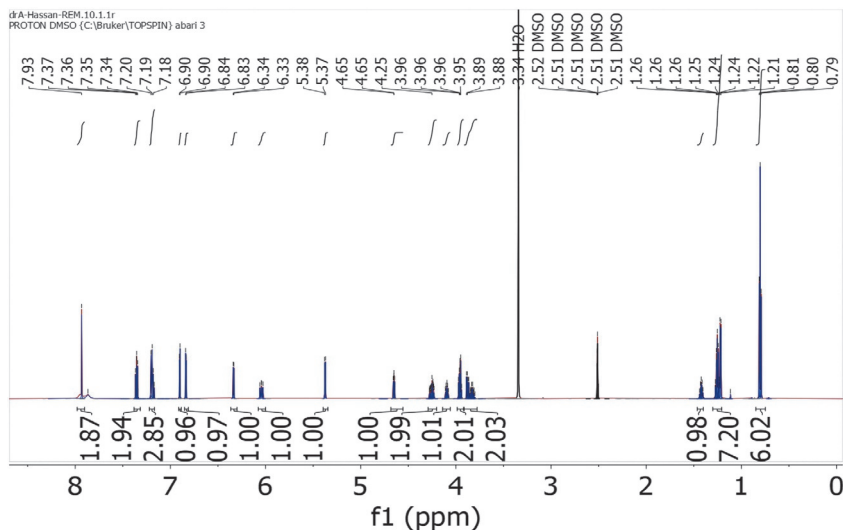
Fig. 6 ^{1}H NMR spectrum of Remdesivir.
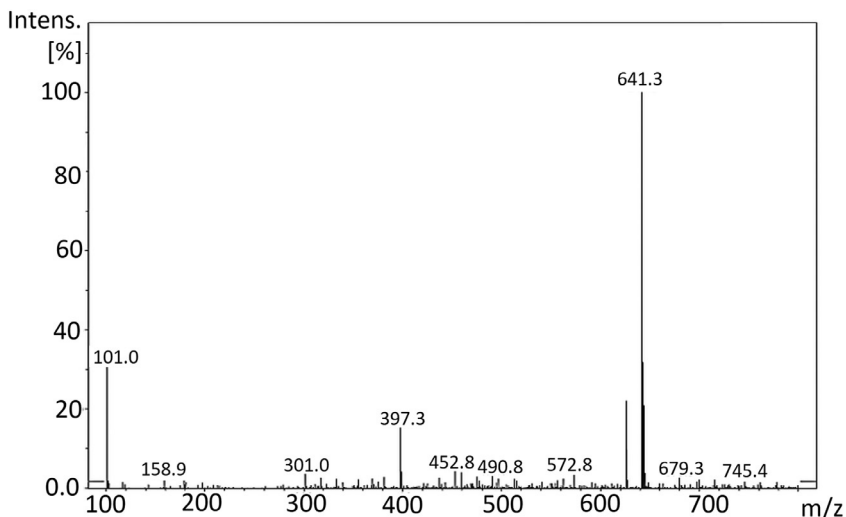
Fig. 7 Full scan mass spectra of Remdesivir.

on the ions intensities– with mobile phase. Flow rate was $0.4\,mL\,min^{-1}$, run time was 5 min. MS parameters were optimized for each compound. The scan was ultra–scan mode. MS2 scans were performed in the mass range of m/z 50–1000. The ESI was operated in positive mode. The source temperature was set to $350\,°C$ nebulizer gas pressure of 55.00 psi; dry gas flow rate of 12.00 L min. Fig. 7 showed the peak at $m/z = 625.6\ [M+23]^{+}$
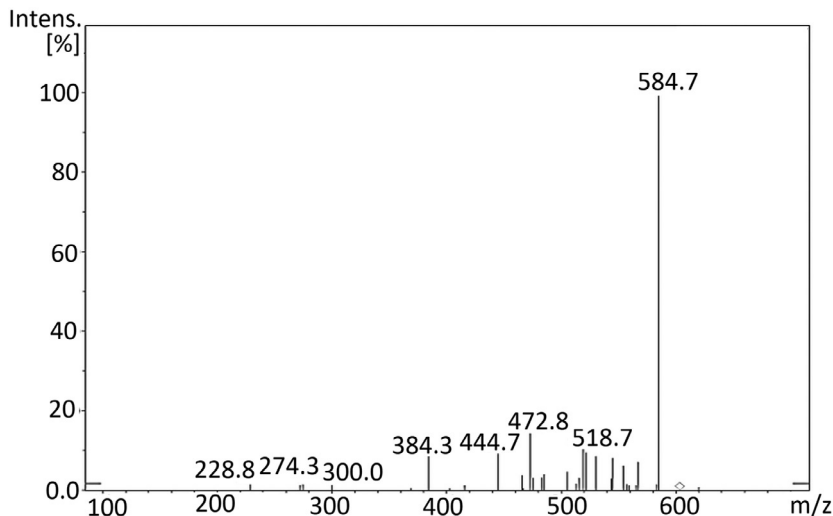
Fig. 8 Product ion spectra of Remdesivir.

due to $[M+Na]^+$ and the peak corresponding to $[M+K]^+$ appeared at 641.3 $[M+39]^+$. Fig. 8 showed the product ion spectra of Remdesivir.

6. Analytical profiles of drug substances and excipients

6.1 Compendial methods of analysis

The compendial monograph (pharmacopoeia) was not reported up to date.

6.2 Titrimetric methods of analysis

6.2.1 Non-aqueous titration

WHO propose a Remdesivir draft for inclusion for The International Pharmacopoeia [19]. They described a Non-aqueous titration method as assay of Remdesivir. Dissolving 0.4 g in 50 mL of glacial acetic acid and titrate with perchloric acid (0.1 mol/L). Each mL of perchloric acid (0.1 mol/L) is equivalent to 60.26 mg of Remdesivir.

6.2.2 Multiple isothermal titration calorimetry (ITC)

Researchers from the University of Spain and USA conducted multiple isothermal titration calorimetry (ITC) measurements and computational molecular dynamics simulations to perform a structural and thermodynamic study of the interaction between CAPTISOL and neutral or protonated Remdesivir. At pH 3, according to the results of the global analysis of the calorimetric measurements, a relatively strong complex with an association

constant of 104 is generated. As a result of the potential of mean force (PMF) profiles, the values obtained for the association constants indicate that the binding is weaker for the structure with the lowest number of sulfobutylether (SBE) substitutions, which is consistent with the ITC conclusion that the affinity is significantly dependent on the number and location of structures containing CAPTISOL [20].

6.3 Electrochemical methods of analysis

The Remdesivir anti–COVID-19 medication electrochemical determination was analyzed theoretically for the first time. An anodic method utilizing the Squaring Dye—Ag_2O_2 combination was investigated in this study. The electroanalytical process's mechanism is branched, implying a rather dynamic nature. However, a mathematical model study based on linear stability theory and bifurcation analysis shows that the composite electroanalytical efficiency as an electrode modification is true, even though it is an electrode modification [18].

6.4 Spectroscopic methods of analysis

6.4.1 Spectrophotometry

Bulduk and Akbel [21] developed and verified UV spectrophotometric techniques for quantifying Remdesivir in pharmaceutical formulations. The UV spectra was recorded between 200 and 800 nm using deionized water as the solvent, and the wavelength of 247 nm was chosen. These techniques were verified in accordance with the protocols outlined in the ICH Q2 standards (R1). The approaches performed well in terms of linearity, accuracy, and recovery. Within a dosage range of 10–60 mg mL^{-1}, correlation values were better than 0.999.

6.4.2 Spectrofluorimetry

Elmansi et al. [22] developed and validate a spectrofluorimetric method for determination of Remdesivir in an Iv infusion and human plasma Measurement of Remdesivir was based on its natural fluorescence at pH 4 and wavelengths of 244/405 nm. Over the range of 1.0–65.0 ng/mL, calibration was accomplished. To obtain maximal sensitivity, different factors impacting the suggested approach were investigated, with detection and quantification limits of 0.287 and 0.871 ng/mL, respectively. The described approach is thought to be the first spectrofluorimetric method for Remdesivir estimation. The approach was also used to determine the drug's concentration in a designed IV infusion and spiked human plasma.

6.5 Chromatographic methods of analysis

6.5.1 Thin-layer chromatography-densitometric (TLC-densitometric)

Noureldeen et al. [23] proposed and validated a green densitometric method for determination of Remdesivir and Favipiravir in pharmaceutical formulations and spiked human plasma on normal phase TLC plates. The developing mobile phase system is ethyl acetate–methanolammonia (8:2:0.2 by volume). Remdesivir and Favipiravir have retardation factors (R_f) of 0.18 and 0.98, respectively. An ICH–approved validation study was conducted. They have outstanding sensitivity with quantitation limits of 0.12 and 0.07 μg/band. Applicable to tablet formulations and spiked plasma, the new approach yielded excellent recoveries between 97.21% and 101.31% the method's greenness was assessed using the Greenness Profile and EcoScale. There are four green profile quadrants and an Eco-Scale score of 80.

6.5.2 High performance liquid chromatography

In The WHO proposal monograph of Remdesivir [19], an HPLC method was described for the determination of Remdesivir and its related compounds in the finished product using a stainless steel column (4.6 mm × 25 cm) packed with end-capped particles of silica gel with chemically-bonded octadecylsilyl groups (5 μm). The mobile phase was a mixture of 35 volumes of phosphoric acid solution and 65 volumes of methanol and operate at a flow rate of 1.0 mL per minute, conducted with a UV spectrophotometer with a wavelength of 237 nm as a detector. A constant temperature of 25 °C was maintained in the column. For standard and test solutions, 5 μL each were injected and recorded in the chromatogram for 25 min. The percentage content of $C_{17}H_{35}N_6O_8P$ was calculated in the sample using the stated content of $C_{17}H_{35}N_6O_8P$ in Remdesivir and the areas of the peaks corresponding to Remdesivir obtained in the chromatograms of standard and test solutions.

In the DAICEL Chiral Technologies proposal analytical methods of Remdesivir, Umstead [24] described an HPLC method for chiral separation and determination of Remdesivir and several of its key-starting materials in final product. A CHIRALPAK® IA-3 (250 mm × 4.6 mm i.d.) column was used, with a mixture of (n-Hexane:Ethanol:IPA:Ethanolamine:Formic acid) (80:5:15:0.05:0.1) (v/v/v/v/v) as a mobile phase and operated at a flow rate of 1.5 mL/min. A UV spectrophotometer was utilized with a wavelength of 245 nm ref. 450 nm as a detection wavelength. A constant temperature of

40 °C was maintained in the column. A standard solution (1.0 mg/mL) was prepared in (Hexane:Ethanol) (50/50) (v/v) and 10 µL was injected each and the chromatogram was recorded for 40 min.

In the Waters proposal, Remdesivir's analytical methods were investigated for separation and determination of Remdesivir to monitor biotransformation events.

Alden et al. [25] described liquid chromatography paired with optical detection or with mass spectrometric method for nucleotide analogs separated using tributylamine as an ion pairing reagent. An Atlantis PREMIER BEH C18 AX 1.7 mm Column (2.1 × 50 mm) was used. The incremental gradient elution was used to separate mixed analytes with polarities that range across a wide range in a single run. Chromatographic mobile phases were produced on-line with IonHance buffer concentrates (which include 20% (v/v) acetonitrile) using a quaternary pump. The buffer concentrates were generated using a 1:5 dilution method to obtain final concentrations of 100 mM in 4% acetonitrile for the IonHance CX-MS Concentrate A, pH 5, and 200 mM in 4% acetonitrile for the IonHance Ammonium Acetate pH 6.8 Concentrate. To create the gradient, the 1:5 dilutions were combined with 18 M water and acetonitrile. The final gradient was 5 mM ammonium acetate (pH 6.8) in 0% acetonitrile to 20 mM ammonium acetate (pH 6.8) in 60% acetonitrile in 4 min using a linear gradient, followed by a 0.5-min return to the initial concentration. Additionally, a longer 8-min gradient was tested with favorable results. and run at 0.5 mL/min. Detector 1 is an Acquity Premier PDA Detector. Detector 2 is an ACQUITY QDa Mass Detector. Maintain the column and samples at 50 °C and 12 °C, respectively, at all times.

Reddy et al. [26] used high–performance liquid chromatography with an ultraviolet detector to develop an unique validated liquid chromatographic method for the quantitative measurement of degradation products in Remdesivir Injectable Pharmaceutical Products. An octyldecylsilane chemically bonded column (Kromasil KR100-5 C18; USP L1 phase) with dimensions of 250 mm length, 4.5 mm inner diameter, and 5 µm particle size was used to improve the procedure. The method was validated in accordance with current regulatory criteria for analytical method validation, including the International Conference on Harmonization. In concentrations ranging from quantification level to 200% of the specification level of specified and unknown degrading contaminants. The method was successfully used to investigate degradation products in Remdesivir Injectable medicinal products.

Patel et al. [27] created a reverse phase high performance liquid chromatographic (RP-HPLC) technique for separation and quantification of Remdesivir in its API form. The separation was performed using a C18 (250 mm × 4.6 mm, 5 µ) column with Buffer, pH 5.0: Acetonitrile (30:70) as the mobile phase at a flow rate of 1 mL/min and detection at 253 nm. The retention time of the drug was 4.402-min. The method's linearity, accuracy, and precision were found to be within the accepted range. Remdesivir has a linearity of 10–30 µg/mL. The drug was exposed to stress conditions of hydrolysis, oxidation, photolysis, and thermal degradation; significant deterioration was identified in alkaline degradation.

6.5.3 Ultra performance liquid chromatography-tandem mass spectrometer (UPLC-MS/MS)

After a one-step protein precipitation process, a HPLC–MS/MS technique was established to quantify active metabolite of Remdesivir (GS-441524 (Nuc)) in rat plasma samples by Du et al. [28]. Under gradient elution conditions, the mobile phase A (ACN:water ratio of 95:5, v/v, 0.1% formic acid) and phase B (water:ACN ratio of 99:1, v/v, 0.1% formic acid) were made fresh. To obtain the baseline separation, the following gradient elution protocol was used: 1.2 min, 99% B; 1.2–3.5 min, 5% B; 3.5–3.6 min, 99% B; 3.6–4.5 min, 99% B. To eliminate the possibility of carryover, methanol:water (1:1, v/v) was utilized. Chromatographic separation was achieved on a Waters XBrige C_{18} column (50 × 2.1 mm, 3.5 µm) with a 4.5-min running time. In electrospray positive ion mode, several reaction monitoring transitions for Nuc were m/z 292.2 → 163.2 and 237.1 → 194.1 for the internal standard (carbamazepine). Maintain a constant temperature of 40 °C in the column. For 1.0 mg/mL solution of GS-441524 (Nuc) solution was prepared in (MeOH:water) (1:1) (v/v), inject 1 µL each and record the chromatogram for 4.5 min. The IS was used to determine Nuc's linearity. The Nuc calibration curve was linear in a range of 2–1000 ng mL^{-1} and a coefficient correlation (r) of greater than 0.990.

Pasupuleti et al. [19] developed analytical method to monitor Remdesivir drug profile in human plasma for pharmacokinetics (PK) and therapeutic drug monitoring (TDM). For the quick detection of Remdesivir in human plasma, the authors present an improved vortex-assisted salt-induced liquid–liquid micro-extraction (VA-SI-LLME) technique in combination with UHPLC-PDA and UHPLC-MS/MS. This procedure entails a single step of precipitating proteins with hydrochloric acid and then extracting with acetonitrile for analysis. Under optimal conditions (500 L acetonitrile + 2.5 g

ammonium sulfate vortex extraction for 2 min), the correlation coefficient of 0.9969 was obtained for UHPLC–PDA (measured at 254 nm) and 0.9990 for UHPLC–MS/MS (measured at electrospray ionization with + ion mode transitions of m/z 603.1 → m/z 402.20 and m/z 603.1 → m/z 199.90). under optimal VA–SI–LLME conditions. The detection and quantification limits for UHPLC/PDA were 1.5 and 5 ng/mL, and 0.3 and 1 ng/mL for UHPLC–MS/MS, respectively. The approach yielded extraction recoveries between 90.79–116.74% and 85.68–101.34% for UHPLC/PDA and UHPLC–MS/MS, respectively, with intraday and interday precision ≤9.59 for both methods.

Avataneo et al. [29] developed UHPLC-MS/MS determination of Remdesivir and GS–441524 in human plasma. Standards and quality controls for Remdesivir and GS–441524 were developed in plasma from healthy donors. Protein precipitation was used to prepare the sample, which was then diluted and injected into the QSight 220 UHPLC-MS/MS apparatus. Chromatographic separation was accomplished using an Acquity HSS T3 1.8 m, 2.1 mm, 50 mm column using a gradient of water and acetonitrile containing 0.05% formic acid. The approach was verified in accordance with EMA and FDA regulations. There was a perfect fit between calibration curves and regression models that were "linear through zero". A 1/x weighting factor was used to make sure that the results were accurate at low concentrations, as well. Calculation coefficients (r^2) were all above 0.998 in all of the calibration curves.

The concentrations of RDV, GS-704277, and GS-441524 in plasma were measured by Humeniuk et al. [30] utilizing a liquid chromatography tandem mass spectroscopy approach with multiple reaction monitoring and electrospray ionization in the positive mode (QPS; LLC) (Newark, DE, USA). Multiple reaction monitoring was used to quantify the transitions m/z 603.3 → 402.2 and m/z 606.3 → 402.2 for RDV and an isotopically labelled internal standard (GS829143), m/z 441.1 → 150.1 and m/z 444.1 → 150.1 for GS-704277 and an isotopically labelled internal standard (GS829466), and m/z 292.2 → 202.2 and m/z 295.2 → 205.2 for GS-441524. The bioanalytical approach was validated using calibrated concentration ranges of 4–4000 ng/mL for RDV, 2–2000 ng/mL for GS-704277, and 2–2000 ng/mL for GS-441524. Inter-assay precision, as measured by coefficient of variation, was 2.1–5.3% for Remdesivir, GS-704277, and GS-441524, and accuracy, as measured by inter-assay percent relative error, was 9.8 to 9.5% for RDV, GS-704277, and GS-441524. All samples were evaluated within the interval specified by data on frozen stability storage.

For the quantification of Remdesivir and its active metabolites GS-441524, Alvarez et al. [31] developed and validated a method that relied on liquid chromatography coupled to triple quadrupole mass spectrometry detection and used 50 μL of plasma to detect the presence of Remdesivir and its active metabolites. A straightforward protein precipitation was performed using 75 μL methanol containing the internal standard (IS) Remdesivir-13C6 and 5 μL 1 M ZnSO$_4$. Following separation on a Kinetex® 2.6 μm Polar C18 100A LC column (100 2.1 mm i.d.), both chemicals were identified using electrospray ionization in positive mode on a mass spectrometer. For Remdesivir, the ion transitions were m/z 603.3, →m/z 200.0, and m/z 229.0; for GS-441524, the ion transitions were m/z 292.2, →m/z 173.1, and m/z 147.1; and for Remdesivir-13C6, the ion transitions were m/z 609.3→ m/z 206.0. The calibration curves for Remdesivir were linear in the 1–5000 g/L range and for GS-441524 were linear in the 5–2500 μg/L range, with the limit of detection set at 0.5 and 2 μg/L and the limit of quantification set at 1 and 5 g/L, respectively. Precisions for Remdesivir at 2.5, 400, and 4000 μg/L and for GS-441524 at 12.5, 125, and 2000 μg/L were less than 14.7% and accuracy was in the [89.6–110.2%] range. There was a minor matrix effect identified, which was accounted for by IS. On NaF-plasma, Remdesivir and its metabolite were shown to be more stable. After 200 mg IV single injection, Remdesivir concentrations immediately fell with a half-life of less than 1 hour, but GS-441524 concentrations increased fast and gradually decreased until H24 with a half-life of about 12 h.

Hu et al. [32] developed a high-performance liquid chromatography-tandem mass spectrometric method in a positive electrospray ionization mode for separating the active metabolite Remdesivir nucleotide triphosphate (RTP) from its precursor Remdesivir nucleotide monophosphate (RMP) using a BioBasic AX column. Chromatographic retention was tuned stepwise using an anion exchange column and matrix stability was enhanced using 5,5′-dithiobis-(2-nitrobenzoic acid) and PhosSTOP EASYpack, and recovery was raised by dissociating tight protein binding using a 2% formic acid aqueous solution. The technique has a quantitation limit of 20 nM for RMP and 10 nM for RTP. Validation of the method indicated appropriate precision (RSD 11.9% for RMP, RSD 11.4% for RTP) and accuracy (93.6%–103% for RMP, 94.5%–107% for RTP).

Xiao et al. [33] established and validated LC-MS/MS techniques for the measurement of Remdesivir and its metabolites GS-441524 and GS-704277 in human plasma. These methods incorporated two critical characteristics to ensure their precision, accuracy, and robustness. Stability difficulties with

the analytes were addressed by treating plasma samples with diluted formic acid (FA) and each analyte was injected separately using distinct ESI modes and organic gradients to maximize sensitivity and reduce carryover. Chromatographic separation was accomplished with a 3.4 min run time on an Acquity UPLC HSS T3 column (2.1 × 50 mm, 1.8 μm). For Remdesivir, GS-441524, and GS-704277, the calibration ranges were 4–4000, 2–2000, and 2–2000 ng/mL, respectively. Across three QC levels, the intraday and interday precision (percent CV) for all three analytes was less than 6.6%, and the accuracy was less than 11.5%. Remdesivir, GS-441524, and GS-704277 plasma can be stored for 392, 392, and 257 days at a temperature of 70 °C for a long time.

Reckers et al. [34] established and validated an LC-MS/MS technique for quantifying Remdesivir, its metabolite GS-441524, and dexamethasone. The approach was applied to 23 blood samples from seven individuals with severe COVID-19. The detection limits for Remdesivir, GS-441524, and dexamethasone were 0.0375 ng/mL, 0.375 ng/mL, and 3.75 ng/mL, respectively. The levels of Remdesivir, GS-441524, and dexamethasone showed modest intra-patient variability but high inter-patient variability. The considerable inter-patient variability emphasizes the significance of therapeutic medication monitoring and probable dosage adjustments in COVID-19 patients in order to achieve effectiveness.

7. Determination of the drug in body fluids and tissues
7.1 Chromatographic methods

Warren et al. [35] developed a LC-MS/MS method for determination of the metabolites (GS-5734) concentration in the intracellular. The LC-MS/MS analysis was carried out utilizing low-flow ion-pairing chromatography, as described in Ref [36]. Analytes were separated using a 50 mm × 2.5 m Luna C_{18}(2) HST column (Phenomenex) linked to an LC–20ADXR ternary pump system (Shimadzu) and an HTS PAL auto-sampler (LEAP Technologies). A multi-stage linear gradient from 10% to 50% acetonitrile in a mobile phase containing 3 mM ammonium formate (pH 5.0) and 10 mM dimethylhexylamine was used to separate analytes over an 8-min period at a flow rate of 150 μL min^{-1}. The detection was carried out using a positive ion and multiple reaction monitoring mode on an API 4000 (Applied Biosystems) MS/MS. The intracellular metabolites alanine metabolite, Nuc, nucleoside monophosphate, nucleoside diphosphate, and nucleoside triphosphate were measured using seven-point standard curves ranging

from 0.274 to 200 pmol (about 0.5 to 400 μM) in untreated cell extract. Adenosine nucleotide levels were also measured to ensure that no dephosphorylation occurred during sample collection and preparation. A Countess automatic cell counter (Invitrogen) was used to count the total number of cells in each sample for determination of the metabolites concentration in the intracellular.

For plasma analysis, Using 20 nM 5-(2-aminopropyl)indole as an internal standard, aliquots of 25 μL each plasma sample were treated with 100 μL of 90% methanol/acetonitrile mixture and 10% water. On the other hand, the Agilent Captiva 96 well 0.2 μm filter plate was used to filter the samples. Filtered samples were dried completely for 20 min and reconstituted with 1% acetonitrile, 99.9% water, and 0.01% formic acid. Using an HTC Pal auto-sampler, an aliquot of 10 μL was injected for LC-MS/MS. Waters Acquity extreme performance LC (Waters Corporation, Milford, MA, USA) was used to separate the samples on a Phenomenex Synergi Hydro-RP 30A column (75 $\times$ 2.0 mM, 4.0 μm) with an analytical flow rate of 0.26 mL min^{-1} and a gradient from Mobile Phase A to Mobile phase B containing 0.2% formic acid in 99% water and 1% acetonitrile over 4.5 min. An electrospray probe on a Waters Xevo TQ-S was employed for MS/MS analysis. Calibration curves with eight points covering over three orders of magnitude in concentration were used to determine plasma levels of GS-734, alanine metabolism product, and nucleoside metabolite (Nuc). To ensure accuracy and precision within 20%, quality control samples were taken at the start and end of the run.

8. Stability
8.1 Stability indicating method

For the measurement of Umifenovir and Remdesivir in tablet dosage form, a simple stability indicating reverse-phase high performance liquid chromatographic (RP-HPLC) approach has been devised by Surabhi and Jain [17]. Using the reference solution, the chromatographic solution was optimized. The chromatographic method employed a Zorbax SB C18 column of dimensions 150 $\times$ 4.6 mm, 3.5 μm, employing isocratic elution with an acetonitrile and water mobile phase in a 50:50 ratios for the chromatographic separation, which was monitored at a wavelength 230 nm PDA detector with a flow rate of 1 mL/min. The duration time of the run was ten minutes. The developed technique was validated in accordance with the ICH recommendations. The calibration curves plotted were linear, with a regression

coefficient of R^2 greater than 0.999, indicating that the linearity was within the limit. As part of technique validation, recovery, specificity, linearity, accuracy, robustness, and ruggedness were determined, and the findings were and found to be within acceptable limits. All of the degradation products produced under the stress conditions are effectively separated, and the peaks have been successfully resolved with an appropriate retention time.

Remdesivir stability–indicating study was developed by Hamdy et al. utilizing HPLC technique [37]. For a chromatographic separation, C_{18} column (250 mm, 5 mm, 5 nm) was used with diode array detection and fluorescence detection. Acetonitrile and distilled water (acidified with phosphoric acid, pH 4) in the ratio of 55:45 (v/v) were employed for isocratic elution. HPLC-diode array detection had a linearity range of 0.1–15 μg/mL, whereas fluorimetric detection had a linearity range of 0.05–15 μg/mL. Accelerated alkaline, acidic, neutral hydrolysis, oxidative, heat, and photolytic stress conditions are all listed by the International Conference on Harmonization as degrading Remdesivir. This study confirm that the parent molecule has been degraded. The proposed approaches were able to identify the intact drug with no overlapping peaks in any of the assumptions that they were based on. Drug stability is endangered by heat and basic hydrolytic stresses, as demonstrated by extensive degradation.

8.2　Solid-state stability

According to ICH requirements, two commercial and two pilot scale batches of Remdesivir were stored in the planned commercial packaging for up to 48 months at 30 °C/75 °RH and for up to 6 months at 40 °C/75 °RH. These included appearance, moisture, assay, and impurity content. For up to 48 months, there was no loss in assay or rise in impurity content. Some batches showed a slight increase in water content between the first and third months, although this remained stable for up to 48 months. An ICH Q1B Photostability Testing of New Drug Substances and Products was performed on one pilot batch. Appearance, assay, impurity, and water content were assessed. The results show Remdesivir is not photolabile.

Stress studies were conducted at −20 °C for one month, 50 °C/ambient humidity for two weeks, and 60 °C/ambient humidity for 1 week to assess shipping and handling conditions. The appearance, assay, impurity content, and water content of samples were all determined. Observed little to no change Remdesivir is therefore stable for 1 month at −20 °C, 2 weeks at 50 °C, and 1 week at 60 °C. [13]. Stability studies were performed according

to current ICH guidelines; Sterility and bacterial endotoxin testing also were performed. Photostability studies are adequately conducted and show that the proposed finished product is photostable. Thus, a shelf-life of 12 months with a storage restriction "store at 2–8 °C" is acceptable based on provided data for Concentrate for Solution for Infusion and the proposed shelf-life of 3 years is accepted for the 100 mg powder for concentrate for solution for infusion [13].

8.3 Solution-phase stability

The prepared diluted solution of Remdesivir is stable for 24 h at room temperature (20–25 °C) or 48 h at refrigerated temperature (2–8 °C) [38].

9. Pharmaceutical applications

Remdesivir (Veklury) has been authorized by the US Food and Drug Administration for use in adult and pediatric patients 12 years of age and weighing at least 40 kg (approximately 88 pounds) for the treatment of COVID-19 that requires hospitalization [29]. In addition, it can be used for other viral infection like Ebola [39].

10. Pharmacology

10.1 Pharmacodynamic properties

Remdesivir is activated intracellularly to create GS-443902 (an adenosine triphosphate analog) which has broad-spectrum action and specifically inhibits viral RNA polymerases. Remdesivir is activated intracellularly via hydrolase cleavage by carboxylesterases, resulting in the formation of GS-704277, an intermediate metabolite. Following the breaking of the phosphoramidate bond, the nucleoside analogue monophosphate, GS-441524-MP, is formed, which is then phosphorylated to provide the pharmacologically active nucleoside triphosphate, GS-443902. When GS-441524-MP is dephosphorylated, the nucleoside analog, GS-441524, is formed, which is less effective in re-phosphorylation. Remdesivir's intracellular metabolic route is represented in Fig. 9. Remdesivir and its metabolites (GS-704277 and GS-441524) can be detected in plasma, but the active triphosphate GS-443902 can only be detected intracellularly, with PBMCs serving as a clinical surrogate cell type for measuring activation of the active triphosphate GS-443902 [30] (Table 6).
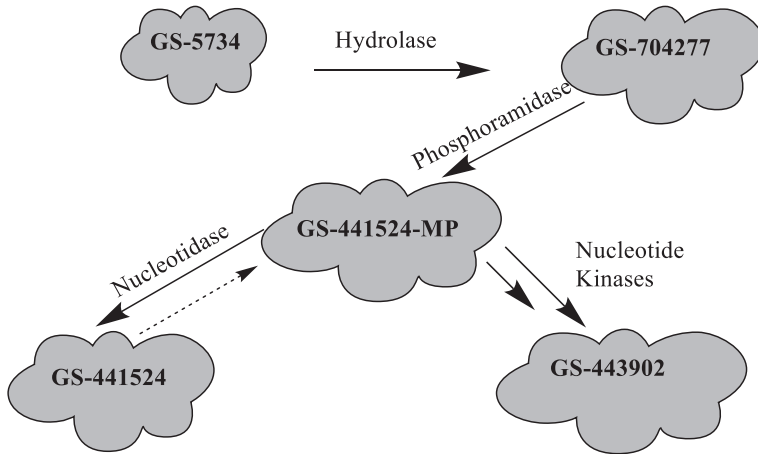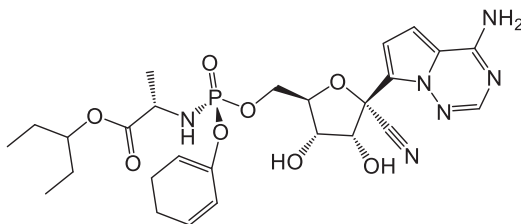
Fig. 9 Intracellular metabolic pathway of Remdesivir.
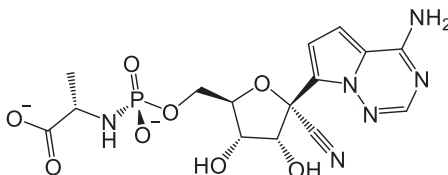
10.1.1 Mechanism of action

Remdesivir is a phosphoramide prodrug of the nucleoside adenosine C. When a medication is injected into the respiratory epithelial cells in the body, it is converted into its active form, nucleoside triphosphate, since it is a prodrug. The active form of Remdesivir can inhibit several coronaviruses from replicating in lung epithelial cells. SARS-CoV-2 is an enclosed, positive-sense, single-stranded RNA virus that is dominated by RNA–dependent RNA polymerase (RdRp), which is coded by the virus itself. After the virus infects the host cell, the viral genomic RNA is employed as a template, and RdRp is translated via the host cell protein synthesis pathway. RdRp is continually employed to finish the transcriptional synthesis of negative-strand subgenomic RNA, the production of numerous structural protein–related mRNAs, and viral genomic RNA replication. RdRp can accurately and effectively generate tens of thousands of nucleotides, allowing all other biological functions to occur after the virus has infected the host cell. The majority of anticoronavirus medicines that target RdRp are nucleoside analogues. The amount of viral RNA produced is reduced as a result. The prodrug is still being studied to see if it terminates RNA chains or induces mutations in the RNA. It was widely known that the prodrug Remdesivir hindered the function of RNA–dependent RNA polymerase, resulting in the elongation of the produced chain, based on Ebola virus investigations [40].

Table 6 The mean metabolites of Remdesivir [30].

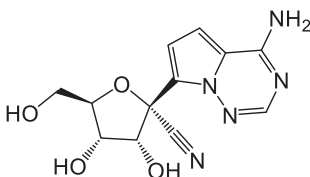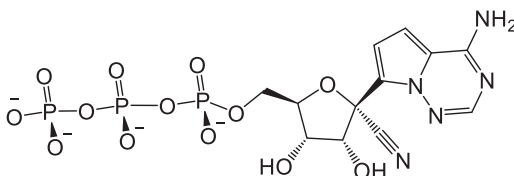| Metabolites code	Metabolites structure
GS–5734	
GS–704277	
GS–441524–MP	
GS–441524	
GS–443902	
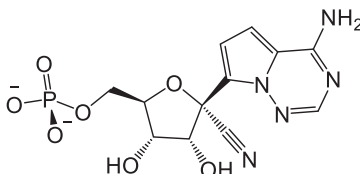
10.1.2 Clinical efficacy and safety

Angamo et al. [41] discovered that Remdesivir therapy resulted in a 21% improvement in clinical recovery rate on day 7 and a 29% rise on day 14. In addition, compared to the control group, Remdesivir-treated patients

had a 39% lower risk of mortality on day 14; however, there was no meaningful difference on day 28. They also found that, despite a conditional recommendation against its use, Remdesivir was still effective in improving early clinical outcomes, reducing early mortality, and avoiding the use of high-flow supplemental oxygen and invasive mechanical ventilation in COVID-19 patients who were hospitalized. In comparison to placebo, Remdesivir was well tolerated with no notable Serious Adverse Effects (SAEs).

In another investigation, Lou et al. [42] found 5 RCT meta-analyses including 1782 individuals with COVID-19. Remdesivir outperformed the placebo-controlled group in terms of clinical improvement (relative risk (RR) = 1.17, 95% confidence interval (CI) = 1.07–1.29, $P = 0.0009$). The results of the Single-Arm Study Meta-analysis are listed below. During treatment of COVID-19 with Remdesivir, the pooled prevalence of clinical improvement meaningful results was 62%. During treatment of COVID-19 with Remdesivir, the incidence rates of acute renal damage, elevated hepatic enzymes, any significant adverse event, and death were 5% and 13%, respectively.

10.2 Pharmacokinetic properties

Deb et al. [43] discovered that the pharmacokinetic (PK) features of the parent Remdesivir, nucleoside core (GS-441524), and alanine metabolite (GS-704277) have been investigated in a limited number of clinical investigations. One of the trials used two highly infected COVID-19 patients in a PK study of the parent Remdesivir and nucleoside core, providing a 200 mg/day loading dose followed by 100 mg/day for the next 12 days. Similarly, pharmacokinetic characteristics were reported in a research with healthy volunteers who took 200 mg of Remdesivir per day for the first 4 days, then 100 mg per day for the next 4 days. Remdesivir and GS-441524 attained maximal concentrations in both experiments within 1 h. A peak serum concentration of 3027 ng/mL was attained immediately after intravenous (IV) infusion, followed by a rapid decline in plasma concentrations after 1 h. The parent Remdesivir's area under the curve (AUC) in 24 h ranged from 2.9 to 4.0 µg h/mL. The pharmacokinetic parameters of GS-441524 differed from those of Remdesivir. Patient 1 and patient 2 had plasma concentrations of 214 ng/mL, 316 ng/mL, and 206 ng/mL, and 113 ng/mL, 184 ng/mL, and 92.6 ng/mL, respectively, 1 h and 4 h after infusion. The AUC of the nucleoside core (GS-441524) has been found to

range from 3.11 to 6.13 µg h/mL after 24 h. On day 1 and day 5, the Remdesivir C_{max} was 5.44 µg/mL and 2.61 µg/mL, respectively, whereas the GS-441524 C_{max} was 0.15 µg/mL and 0.14 µg/mL, respectively. On days 1 and 5, the AUC of parent Remdesivir was 2.92 and 1.56 µg h/mL, respectively, and 2.24 and 2.23 µg h/mL for GS-441524. Single or multiple dosage regimens of Remdesivir were tested for up to 14 days in a complete dose escalation trial with healthy participants. Remdesivir (3 mg to 225 mg) was administered as a 2-h IV infusion with a linear kinetics profile. After a single dosage of 3 mg to 225 mg Remdesivir, the C_{max} varied from 57.5 ng/mL to 4420 ng/mL, with each dose requiring 2 h to reach the peak plasma concentration. The AUC was also varied, ranging from 67.1 ng/mL to 5260 ng/mL. The clearance and volume of distribution, respectively, varied from 755 to 719 mL/min and 45.1 to 66.5 L. C_{max} and AUC showed similar dose-dependent patterns for GS-441524 and GS-704277 as well. In comparison to in vitro EC50 values found in SARS-CoV-2 experimental models, active triphosphate cellular concentrations were much greater (220–370-fold) following 75 mg or 150 mg single IV administration. Interestingly, the PK parameters of the parent Remdesivir prodrug at 150 mg/day for 7 or 14 days were comparable. However, between day 1 and day 7 or 14, the GS-441524 and GS-704277 were slightly different. Following daily dosing, the alanine metabolite raised by around 1.9-fold.

With just a few studies of Remdesivir PK in COVID-19 patients with renal failure, the present understanding of Remdesivir in particular populations such as renal or hepatic impairment is quite limited. In silico modeling of Remdesivir, pharmacokinetics suggests that its distribution is influenced by age, weight, liver, and renal function status. Because Remdesivir and its active metabolite are eliminated in the urine, dosage assessment data on individuals with renal impairment is required. Remdesivir plasma concentrations are higher in people with chronic renal disease. Healthy volunteers and renally compromised patients had 2.5- to 4-fold differences in critical PK characteristics of parent Remdesivir, such as AUC0-infinity, C_{max}, clearance, and volume distribution. Remdesivir should not be administered to individuals with an eGFR of less than 30 mL/min, according to the FDA. However, acute kidney damage was one of the most common side events in two clinical studies with Remdesivir. The solubility enhancer sulfobutylether-cyclodextrin sodium (SBECD) in Remdesivir's formulations may be to blame for the drug's renal impairment. SBECD is present in a variety of renally toxic medications (e.g., the IV formulation of voriconazole) and is excreted by the kidneys,

with buildup occurring at CrCl 50 mL/min. SBECD, despite its buildup in renally compromised individuals, does not appear to induce significant renal damage, according to research. When using Remdesivir, it's still a good idea to keep an eye on your kidney function. Remdesivir, it turns out, can reduce the inflammatory response in mice with non–alcoholic fatty liver disease (NAFLD) caused by a high-fat diet. The primary theme of Remdesivir-mediated blockage of NAFLD development has been identified as the reduction of stimulator of interferon genes (STING), an endoplasmic reticulum membrane protein implicated in innate immune response. This raises the possibility that obese people with COVID-19 and liver disease may benefit from Remdesivir treatment in two ways, potentially affecting Remdesivir disposition, therapy, and safety.

10.3 Dosing

10.3.1 Adults and adolescents (≥12 years of age and weighing ≥40 kg)
Patients admitted to the hospital should receive a 200 mg intravenously infusion once, followed by a 100 mg intravenously infusion once-daily for 4 days (duration can be prolonged for an additional 5 days if there is no clinical response), or 10 days if the patient requires mechanical breathing and/or ECMO [44].

10.3.2 Pediatrics (<12 years of age or weighing <40 kg)
For patients of the pediatric weighing between 3.5 kg and 40 kg, the suggested dosage is a single loading dose of VEKLURY 5 mg/kg on Day 1, followed by VEKLURY 2.5 mg/kg once day starting on Day 2. For pediatric patients younger than 12 years of age and weighing at least 40 kg, a single loading dose of 200 mg on Day 1 is suggested, followed by once-daily maintenance doses of 100 mg starting on Day 2.

10.3.3 Geriatrics (>65 years of age)
Patients above the age of 65 years do not require any dose adjustments when using VEKLURY [45,46].

10.3.4 For renal impairment
- Remdesivir has not been subjected to a rigorous study in patients suffering from renal impairment [44].
- In patients with poor renal function (eGFR 30 mL/min), Remdesivir is not indicated due to the possibility of accumulation of sulfobutylether–cyclodextrin (SBECD), the excipient in the medication (this is the same issue with voriconazole IV). Nevertheless, many experts (including the

JH ABX Guide) support use due to the absence of significant toxicity when administered (voriconazole or Remdesivir) [44,46].

10.3.5 Hepatic impairment

VEKLURY's pharmacokinetics in patients with hepatic impairment have not been studied. There is no dose guideline for patients with hepatic impairment. VEKLURY should not be initiated in patients with an ALT level greater than five times the upper limit of normal [45,46].

10.4 ADME profile

ADME: IV Administration

10.4.1 Absorption

According to Deb et al. [43] study, Remdesivir comes in two different forms: a solution and a lyophilized powder. The solution is supplied in a 100 mg/20 mL vial with a 5 mg/mL concentration, and the lyophilized powder is packaged in a single-dose vial with a concentration of 100 mg. A 0.9% saline or a 5% glucose solution must be used to reconstitute the powder formulation. Intravenous infusion over 30 to 120 min is the most effective form of delivery. Remdesivir is given to adults in the following way: On day one, a 200 mg intravenous loading dose was given, followed by daily IV doses of 100 mg for 2–5 days or up to 10 days. Because intravenous administration allows for 100% absorption of Remdesivir, it is the recommended method. Because of the high hydrolysis-mediated first-pass clearance in the gastrointestinal tract, oral administration is not recommended, resulting in reduced absorption and systemic concentration. Remdesivir has been developed as a prodrug to boost cellular Remdesivir triphosphate concentrations. Intramuscular injection, while better than oral, would still result in subtherapeutic levels since Remdesivir is released slowly from the muscles, leading blood concentrations to fall below therapeutic levels. Since SARS-CoV-2 first targets the lungs, the inhaled route of administration of Remdesivir is now being investigated, and it is assumed that absorption would be sufficient to transport the medicine directly into the primary infected region. The inhaled formulation is primarily intended for outpatient usage and for COVID-19 individuals with less severe symptoms. The Remdesivir prodrug diffuses past the cellular membrane after gradual infusion and undergoes a series of hydrolysis events in the cytoplasm. When the nucleoside core (GS-441524) is hydrolyzed, a more water-soluble monophosphate form is formed, which is unable to go back and hence stays in the infected cells. As a result, when given as a slow intravenous infusion,

the ester prodrug of Remdesivir is well absorbed. Transporters can affect Remdesivir absorption in addition to the dose form and method of administration. P-glycoprotein (P-gp) and organic anion transporting polypeptides 1B1 (OATP1B1) transporters are substrates for Remdesivir. Similarly, Remdesivir's alanine metabolite is an OATP1B1 and OATP1B3 substrate. P-gp can efflux Remdesivir out of the cellular compartment depending on the transporter expression profile in the cell membrane, resulting in reduced intracellular levels and efficacy.

10.4.2 Distribution

According to Deb et al. [43] study, After intravenous administration of Remdesivir, the medication enters the tissues and blood cells via passive diffusion. The parent Remdesivir binds to human plasma proteins with an affinity of 88.0–93.6%, whereas GS-441524 and GS-704277 attach to proteins with 2% and 1%, respectively. Because of its instability within the tissues, Remdesivir is predicted to have a poor tissue distribution; yet, once its active metabolite penetrates the cells, it accumulates more than the extracellular prodrug form. With a single dosage of 10 mg to 225 mg, Remdesivir exhibited a volume of distribution of roughly 45.1–73.4 L in a cohort of eight participants. Similarly, a 7-day or 14-day multiple-dose (150 mg/day) research revealed a volume of distribution of 85.5 L. GS-441524 (nucleoside core) and GS-443902 (active triphosphate) concentrations in peripheral blood mononuclear cells (PBMCs) were utilized as markers of Remdesivir distribution throughout the cellular compartment. It's worth noting that intracellular concentrations were 220 to 370 times greater than the SARS-CoV-2 EC50. There is modest animal evidence of Remdesivir distribution to most tissues in rats and monkeys, but little or no evidence of Remdesivir presence in the brain, indicating that it does not pass the blood–brain barrier well. To attain larger concentrations in the affected organs, higher or more frequent dosage may be required. Remdesivir dosages more than 200 mg, on the other hand, have been connected to hepatotoxicity and renal failure. Thus, additional development of an inhalation dosage form is required so that Remdesivir can be delivered to infected cells at optimal concentrations while minimizing systemic toxicity and adverse medication responses.

10.4.3 Metabolism

In Deb et al. [43] study, Remdesivir is a prodrug that is converted to its active triphosphate form by a hydrolysis process (GS-443902). The prodrug

is metabolized to the degree stated in parenthesis by carboxylesterase 1 (CES1) (80%), cathepsin A (10%), and CYP3A (10%). CYP2C8 and CYP2D6 were also discovered to have a role in the metabolism of Remdesivir in vitro. The Histidine Triad Nucleotide-binding Protein 1 metabolizes GS-704277 (HINT-1). The majority of the metabolites (74%) are identified in urine, while roughly 18% are found in feces. The nucleoside core metabolite (GS-441524) was the most common Remdesivir found in urine, with only 10% of the parent Remdesivir prodrug recovered. Hepatic blood flow, rather than metabolic enzymes, drives Remdesivir clearance; this is thought to be true due to Remdesivir's high extraction ratio and short elimination half-life.

10.4.4 Elimination

According to Deb et al. [43] study, Remdesivir's nucleoside core (GS-441524) is the most prevalent derivative found in urine, with Remdesivir and other metabolites present in moderate to low amounts. Parent Remdesivir and GS-704277 (alanine metabolite) are excreted mostly by biotransformation, but GS-441524 is removed primarily through renal processes such as glomerular filtration and active tubular secretion. Approximately 10% of the parent Remdesivir is excreted as a metabolite in the urine. In contrast, 49% of the dosage is excreted in the urine as GS-441524. In the feces, no Remdesivir or alanine metabolites were found, and only 1% of the dosage was eliminated as the nucleoside core. The half-life of GS-441524 is 27 h, compared to 1 h and 1.3 h for Remdesivir and GS-704277, respectively. The plasma half-life is around 1 h, whereas the intracellular nucleoside triphosphate half-life is 14 to 24 h. Because of its anionic charge, the nucleoside triphosphate stays in the cellular compartment for a longer time. Remdesivir's nucleoside triphosphate nucleoside half-life allows for once-daily dosage. Patients with renal impairment or those receiving renal replacement therapy such as dialysis or hemodialysis should avoid Remdesivir since it is mostly eliminated by the kidneys. Patients with an eGFR of more than 30 mL/min can take Remdesivir without needing to modify their dosage, but once the eGFR falls below 30 mL/min, Remdesivir is no longer indicated.

Acknowledgments

References

[1] J.J. Malin, I. Suárez, V. Priesner, G. Fätkenheuer, J. Rybniker, Remdesivir against COVID-19 and other viral diseases, Clin. Microbiol. Rev. 34 (1) (2020). p. e00162-20.

[2] Y. Pashaei, Analytical methods for the determination of remdesivir as a promising antiviral candidate drug for the COVID-19 pandemic, Drug Discov. Ther. 14 (6) (2021) 273–281.

[3] Remdesivir (Compound), 2022. [cited 2022 24 March]; from https://pubchem.ncbi.nlm.nih.gov/compound/121304016#section=3D-Conformer.

[4] Remdesivir (HMDB0304869), The Metabolomics Innovation Centre (TMIC), 2022, [cited 2022 24 March]; from https://hmdb.ca/metabolites/HMDB0304869.

[5] Remdesivir, The Merck Index Online 2022, 2022, [cited 2022 24 March]; from https://www.rsc.org/Merck-Index/monograph/m12252/remdesivir?q=unauthorize.

[6] Remdesivir, 2022. [cited 2022 24 March]; from https://www.simsonpharma.com/product/2-ethylbutyl-r-2r-3s-4r-5r-5-4-aminopyrrolo-2-1-f-1-2-4-triazin-7-yl-5-cyano-3-4-dihydroxytetrahydrofuran-2-yl-methoxy-phenoxy-phosphoryl-l-alaninate.

[7] 3QKI37EEHE, 2022. [cited 2022 24 March]; from https://pubchem.ncbi.nlm.nih.gov/substance/328083432.

[8] Remdesivir, ChemSpider Search and Share Chemistry 2022, 2022, [cited 2022 24 March]; from http://www.chemspider.com/Chemical-Structure.58827832.html?rid=afcba29c-0108-40a8-a23b-68f20f7bfb2c&page_num=0.

[9] Remdesivir, Drugs.com updated 2 Mar 2022; from, 2022. https://www.drugs.com/mtm/remdesivir.html.

[10] D. Siegel, H.C. Hui, E. Doerffler, M.O. Clarke, K. Chun, L. Zhang, S. Neville, E. Carra, W. Lew, B. Ross, Q. Wang, L. Wolfe, R. Jordan, V. Soloveva, J. Knox, J. Perry, M. Perron, K.M. Stray, O. Barauskas, J.Y. Feng, Y. Xu, G. Lee, A.L. Rheingold, A.S. Ray, R. Bannister, R. Strickley, S. Swaminathan, W.A. Lee, S. Bavari, T. Cihlar, M.K. Lo, T.K. Warren, R.L. Mackman, Discovery and synthesis of a phosphoramidate prodrug of a pyrrolo[2,1-f][triazin-4-amino] adenine C-nucleoside (GS-5734) for the treatment of Ebola and emerging viruses, J. Med. Chem. 60 (5) (2017) 1648–1661.

[11] T. Vieira, A.C. Stevens, A. Chtchemelinine, D. Gao, P. Badalov, L. Heumann, Development of a large-scale cyanation process using continuous flow chemistry en route to the synthesis of remdesivir, Org. Proc. Res. Dev. 24 (10) (2020) 2113–2121.

[12] K. Kumar Palli, P. Ghosh, S. Krishna Avula, B.S.S. Rao, A.D. Patil, S. Ghosh, G. Sudhakar, C.R. Reddy, P.S. Mainkar, S. Chandrasekhar, Total synthesis of remdesivir, Tetrahedron Lett. (2021), 153590.

[13] EMEA, Assessment report—Veklury, Procedure No. EMEA/H/C/005622/0000, 2020. 25 June 2020; from https://www.ema.europa.eu/en/documents/assessment-report/veklury-epar-public-assessment-report_en.pdf Retrieved October 23, 2021.

[14] S. Sekharan, X. Liu, Z. Yang, X. Liu, L. Deng, S. Ruan, Y. Abramov, G. Sun, S. Li, T. Zhou, B. Shi, Q. Zeng, Q. Zeng, C. Chang, Y. Jin, X. Shi, Selecting a stable solid form of remdesivir using microcrystal electron diffraction and crystal structure prediction, RSC Advances 11 (28) (2021) 17408–17412.

[15] K. Yu, S. Chen, C. Amgoth, G. Tang, H. Bai, X. Hu, Two polymorphs of Remdesivir: Crystal Structure, solubility, and pharmacokinetic study, CrystEngComm 23 (2021).

[16] S. Sahakijpijarn, C. Moon, J.J. Koleng, D.J. Christensen, R.O. Williams Iii, Development of remdesivir as a dry powder for inhalation by thin film freezing, Pharmaceutics 12 (11) (2020) 1002.

[17] S.R. Surabhi, N. Jain, Validated stability indicating method for determination of umifenovir-remdesivir in presence of its degradation products, Int. J. Dev. Res. 11 (2021) 6.

[18] V.V. Tkach, M. Kushnir, S.C. de Oliveira, J. Ivanushko, A.V. Velyka, A.F. Molodianu, P.I. Yagodynets, Z.O. Kormosh, L. Vaz dos Reis, O.V. Luganska, Theoretical description for anti-COVID-19 drug Remdesivir electrochemical determination, assisted by squaraine Dye–Ag$_2$O$_2$ composite, Biointerface Res. Appl. Chem. 11 (2) (2021) 9201–9208.

[19] Organization, W.H, WHO Drug Information 2020, vol. 34, WHO Drug Information, 2021, pp. 862–876. 4 [full issue].

[20] Á. Piñeiro, J. Pipkin, V. Antle, R. Garcia-Fandino, Remdesivir interactions with sulphobutylether-β-cyclodextrins: a case study using selected substitution patterns, J. Mol. Liquids 346 (2022) 117157.

[21] I. Bulduk, E. Akbel, A comparative study of HPLC and UV spectrophotometric methods for remdesivir quantification in pharmaceutical formulations, J. Taibah Univ. Sci. 15 (1) (2021) 507–513.

[22] H. Elmansi, A.E. Ibrahim, I.E. Mikhail, F. Belal, Green and sensitive spectrofluorimetric determination of Remdesivir, an FDA approved SARS-CoV-2 candidate antiviral; application in pharmaceutical dosage forms and spiked human plasma, Anal. Meth. 13 (23) (2021) 2596–2602.

[23] D.A. Noureldeen, J.M. Boushra, A.S. Lashien, A.F.A. Hakiem, T.Z. Attia, Novel environment friendly TLC-densitometric method for the determination of anti-coronavirus drugs "Remdesivir and Favipiravir": green assessment with application to pharmaceutical formulations and human plasma, Microchem. J. 174 (2022) 107101.

[24] W.J. Umstead, The chiral separation of remdesivir and several of its key starting materials, LC-GC North America 39 (6) (2021) 291–293.

[25] B.A. Alden, P. Christensen, D. Foley, L.J. Calton, S. Barnes, G. Gallo, M.A. Lauber, Comprehending COVID-19: Mixed-Mode Chromatography for Ion Pairing Free LC-MS of Remdesivir and Remdesivir Triphosphate, Waters Corporation, 2021.

[26] H.R. Reddy, S.R. Pratap, N. Chandrasekhar, S.Z.M. Shamsuddin, A novel liquid chromatographic method for the quantitative determination of degradation products in remdesivir injectable drug product, J. Chromat. Sci. (2021).

[27] V. Patel, N. Tiwari, K. Patel, Stability indicating RP-HPLC method development and validation for the estimation of Remdesivir in API form, World J. Pharm. Pharmaceut. Sci. 10 (6) (2021) 1544–1551.

[28] P. Du, G. Wang, S. Yang, P. Li, L. Liu, Quantitative HPLC-MS/MS determination of Nuc, the active metabolite of remdesivir, and its pharmacokinetics in rat, Anal. Bioanal. Chem. 413 (23) (2021) 5811–5820.

[29] V. Avataneo, A. de Nicolò, J. Cusato, M. Antonucci, A. Manca, A. Palermiti, C. Waitt, S. Walimbwa, M. Lamorde, G. di Perri, A. D'Avolio, Development and validation of a UHPLC-MS/MS method for quantification of the prodrug remdesivir and its metabolite GS-441524: a tool for clinical pharmacokinetics of SARS-CoV-2/COVID-19 and Ebola virus disease, J. Antimicrob. Chemother. 75 (7) (2020) 1772–1777.

[30] R. Humeniuk, A. Mathias, B.J. Kirby, J.D. Lutz, H. Cao, A. Osinusi, D. Babusis, D. Porter, X. Wei, J. Ling, Pharmacokinetic, pharmacodynamic, and drug-interaction profile of remdesivir, a SARS-CoV-2 replication inhibitor, Clin. Pharmacokinet. (2021) 1–15.

[31] J.-C. Alvarez, P. Moine, I. Etting, D. Annane, I.A. Larabi, Quantification of plasma remdesivir and its metabolite GS-441524 using liquid chromatography coupled to tandem mass spectrometry. Application to a covid-19 treated patient, Clin. Chem. Lab. Med. 58 (9) (2020) 1461–1468.

[32] W. Hu, L. Chang, C. Ke, Y. Xie, J. Shen, B. Tan, J. Liu, Challenges and stepwise fit-for-purpose optimization for bioanalyses of remdesivir metabolites nucleotide monophosphate and triphosphate in mouse tissues using LC–MS/MS, J. Pharmaceut. Biomed. Anal. 194 (2021) 113806.

[33] D. Xiao, K.H. John Ling, T. Tarnowski, R. Humeniuk, P. German, A. Mathias, J. Chu, Y.-S. Chen, E. van Ingen, Validation of LC-MS/MS methods for determination of remdesivir and its metabolites GS-441524 and GS-704277 in acidified human plasma and their application in COVID-19 related clinical studies, Anal. Biochem. 617 (2021) 114118.

[34] S.V. Gandhi, B.G. Kapoor, Development and validation of UV spectroscopic method for estimation of baricitinib, J. Drug Deliv. Ther. 9 (4-s) (2019) 488–491.

[35] T.K. Warren, R. Jordan, M.K. Lo, A.S. Ray, R.L. Mackman, V. Soloveva, D. Siegel, M. Perron, R. Bannister, H.C. Hui, Therapeutic efficacy of the small molecule GS-5734 against Ebola virus in rhesus monkeys, Nature 531 (7594) (2016) 381–385.

[36] L. Durand-Gasselin, K.K. Van Rompay, J.E. Vela, I.N. Henne, W.A. Lee, G.R. Rhodes, A.S. Ray, Nucleotide analogue prodrug tenofovir disoproxil enhances lymphoid cell loading following oral administration in monkeys, Mol. Pharm. 6 (4) (2009) 1145–1151.

[37] M.M.A. Hamdy, M.M. Abdel Moneim, M.F. Kamal, Accelerated stability study of the ester prodrug remdesivir: recently FDA-approved Covid-19 antiviral using reversed-phase-HPLC with fluorimetric and diode array detection, Biomed. Chromatogr. 5 (10) (2021).

[38] FDA, Fact sheet for healthcare providers emergency use authorization (EUA) OF VEKLURY® (remdesivir) for hospitalized pediatric patients weighing 3.5 kg to less than 40 kg or hospitalized pediatric patients less than 12 years of age weighing at least 3.5 kg. 2020, 2021, Available from: Retrieved October 26, 2022 [cited 2022 24 March]. from https://www.fda.gov/media/137566/download.

[39] EMA, Annex I—Conditions of use, conditions for distribution and patients targeted adressed to member states (Remdesivir gilead), 2020. from https://www.ema.europa.eu/en/documents/other/conditions-use-conditions-distribution-patients-targeted-conditions-safety-monitoring-addressed_en-3.pdf Retrieved October 25, 2021.

[40] I. Kumar, A review on pharmacokinetics, pharmacodynamics and clinical aspects of remdesivir and favipiravir for the treatment of coronavirus disease, J. Drug Deliv. Ther. 11 (1) (2021) 121–129.

[41] M.T. Angamo, M.A. Mohammed, G.M. Peterson, Efficacy and safety of remdesivir in hospitalised COVID-19 patients: a systematic review and meta-analysis, Infection (2021).

[42] L. Lou, H. Zhang, Z. Li, B. Tang, Z. Li, The efficacy and safety of remdesivir in the treatment of patients with COVID-19: a systematic review and meta-analysis, medRxiv (2021). p. 2021.03.12.21253470.

[43] S. Deb, A.A. Reeves, R. Hopefl, R. Bejusca, ADME and pharmacokinetic properties of remdesivir: its drug interaction potential, Pharmaceuticals 14 (7) (2021) 655.

[44] K.P.D.B. Dzintars, E.P.D. Avdic, Remdesivir, 2022.

[45] Gilead Sciences Canada Inc., Product monograph: remdesivir for injection; remdesivir solution for injection, 2022, [cited 2022 24 March]; from https://pdf.hres.ca/dpd_pm/00057134.PDF.

[46] Gilead Sciences Ireland UC, Veklury (Remdesivir): EU Summary of Product Characteristics, 2022, [cited 2022 24 March]; from https://www.ema.europa.eu/en/documents/other/veklury-product-information-approved-chmp-25-june-2020-pending-endorsement-european-commission_en.pdf.